Spectral behavior of a terahertz quantum-cascade laser

J.M. Hensley,[1,*] Juan Montoya,[1] and M.G. Allen,[1]
J. Xu,[2] L. Mahler,[2] A. Tredicucci,[2]
H.E. Beere,[3] and D.A. Ritchie[3]

[1]Physical Sciences Inc., 20 New England Business Center, Andover, Massachusetts 01810-1077
[2]NEST-INFM and Scuola Normale Superiore, Piazza San Silvestro 12, 56127 Pisa, Italy
[3]Cavendish Laboratory, University of Cambridge, J J Thomson Avenue CB3 0HE, Cambridge, United Kingdom
**Hensley@psicorp.com*

Abstract: In this paper, the spectral behavior of two terahertz (THz) quantum cascade lasers (QCLs) operating both pulsed and cw is characterized using a heterodyne technique. Both lasers emitting around 2.5 THz are combined onto a whisker contact Schottky diode mixer mounted in a corner cube reflector. The resulting difference frequency beatnote is recorded in both the time and frequency domain. From the frequency domain data, we measure the effective laser linewidth and the tuning rates as a function of both temperature and injection current and show that the current tuning behavior cannot be explained by temperature tuning mechanisms alone. From the time domain data, we characterize the intra-pulse frequency tuning behavior, which limits the effective linewidth to approximately 5 MHz.

OCIS codes: (140.0140) Lasers and laser optics; (140.3070) Infrared and far-infrared lasers.

References and links

1. R. Köhler, A. Tredicucci, F. Beltram, H.E. Beere, E.H. Linfield, A.G. Davies, D.A. Ritchie, R.C. Iotti, F. Rossi, "Terahertz semiconductor-heterostructure laser," Nature **417**, 156–159 (2002).
2. B.S. Williams, S. Kumar, Q. Hu, and J.L. Reno, "High-power terahertz quantum-cascade lasers," Electron. Lett. **42**, 89–90 (2006).
3. C. Walther, M. Fischer, G. Scalari, R. Terazzi, N. Hoyler, and J. Faist, "Quantum cascade lasers operating from 1.2 to 1.6 THz," Appl. Phys. Lett. **91**, 131122 (2007).
4. S. Kumar, Q. Hu, and J.L. Reno, "186 K operation of terahertz quantum-cascade lasers based on a diagonal design," Appl. Phys. Lett. **94**, 131105 (2009).
5. J. R. Gao, J. N. Hovenier, Z. Q. Yang, J. J. A. Baselmans, A. Baryshev, M. Hajenius, T. M. Klapwijk, A. J. L. Adam, T. O. Klaassen, B. S. Williams, S. Kumar, Q. Hu, and J. L. Reno, "Terahertz heterodyne receiver based on a quantum cascade laser and a superconducting bolometer," Appl. Phys. Lett. **86**, 244104 (2005).
6. H. Hübers, S. Pavlov, A. Semenov, R. Köhler, L. Mahler, A. Tredicucci, H. Beere, D. Ritchie, and E. Linfield, "Terahertz quantum cascade laser as local oscillator in a heterodyne receiver," Opt. Express **13**, 5890–5896 (2005).
7. A. A. Danylov, J. Waldman, T. M. Goyette, A. J. Gatesman, R. H. Giles, J. Li, W. D. Goodhue, K. J. Linden, and W. E. Nixon, "Terahertz sideband-tuned quantum cascade laser radiation," Opt. Express **16**, 5171–5180 (2008).
8. S. Barbieri, J. Alton, C. Baker, T. Lo, H. Beere, and D. Ritchie, "Imaging with THz quantum cascade lasers using a Schottky diode mixer," Opt. Express **13**, 6497–6503 (2005).
9. M. Lee, M. C. Wanke, M. Lerttamrab, E. W. Young, A. D. Grine, J. L. Reno, P. H. Siegel, and R. J. Dengler, "Heterodyne Mixing of Terahertz Quantum Cascade Lasers Using a Planar Schottky Diode," IEEE J. Sel. Top. Quantum Electron. **14**, 370 (2008).
10. N. Beverini, G. Carelli, A. De Michele, A. Moretti, L. Mahler, A. Tredicucci, H. E. Beere, and D. A. Ritchie, "Frequency Characterization of a Terahertz Quantum-Cascade Laser," IEEE Trans. Instrum. Meas. **56**, 262–265(2007).
11. A. L. Betz, R. T. Boreiko, B. S. Williams, S. Kumar, Q. Hu, and J. L. Reno, "Frequency and phase-lock control of a 3 THz quantum cascade laser," Opt. Lett. **30**, 1837–1839 (2005).
12. S. Barbieri, J. Alton, H. E. Beere, E. H. Linfield, D. A. Ritchie, S. Withington, G. Scalari, L. Ajili, and J. Faist, "Heterodyne mixing of two far-infrared quantum cascade lasers by use of a point-contact Schottky diode," Opt. Lett. **29**, 1632–1634 (2004).

#116407 - $15.00 USD Received 28 Aug 2009; revised 16 Oct 2009; accepted 19 Oct 2009; published 23 Oct 2009

13. L. Mahler, A. Tredicucci, R. Kohler, F. Beltram, H. E. Beere, E. H. Linfield, and D. A. Ritchie, "High-Performance operation of single-mode terahertz quantum cascade lasers with metallic gratings," Appl. Phys. Lett. **87**, 181101 (2004).
14. L. M. Matarrese and K. M. Evenson, "Improved coupling to a infrared whisker diodes by use of antenna theory," Appl. Phys. Lett. **17**, 8–10 (1970).
15. H. Kräutle, E. Sauter, and G.V. Schultz, "Antenna characteristics of whisker diodes used as submillimeter receivers," Infrared Phys. **17**, 477–483 (1977).
16. S. A. Lourenço, I. F. L. Dias, J. L. Duarte, E. Laureto, L. C. Poças, D. O. Toginho Filho, and J. R. Leite, "Thermal Expansion Contribution to the Temperature Dependence of Excitonic Transitions in GaAs and AlGaAs," Braz. J. Phys. **34**, 517 (2004).
17. M. S. Vitiello, G. Scamarcio, and V. Spagnolo, "Time-resolved measurement of the local lattice temperature in terahertz quantum cascade lasers," Appl. Phys. Lett. **92**, 101116 (2008).
18. C. A. Evans, V. D. Jovanovic, D. Indjin, Z. Ikonic, and P. Harrison, "Investigation of thermal effects in quantum-cascade lasers," IEEE J. Quantum Electron. **42**, 859 (2006).

Introduction

As one of the most efficient sources of coherent terahertz (THz) radiation, the quantum cascade laser (QCL) shows significant promise in enabling THz applications in sensing and imaging. Although since the demonstration of the first THz QCL [1] there has been significant improvement in output power [2], frequency coverage [3], and operating temperature [4], the state of the technology remains such that these devices still emit more average power and operate at higher temperature when driven in pulsed mode rather than cw. However, at the same time, their spectral purity suffers in pulsed mode. In this paper we report on the results of a study of THz QCL spectral behavior under both pulsed and cw drive conditions by beating together the optical output of two similar 2.5 THz QCLs with a Schottky diode mixer.

Coupling a QCL to a THz mixer has been previously demonstrated in a homodyne configuration with a hot electron bolometer (HEB) [5,6] and with a Schottky diode as source [7] and as a detector [8]. Coupling to a Schottky diode integrated with the QCL has also been demonstrated [9]. In a heterodyne configuration, QCLs have been mixed with [10] and stabilized to [11] a far-infrared (FIR) molecular gas laser and with another QCL [12]. In this paper, the spectral behavior of two THz QCLs based on the chirped superlattice design with semiconductor-metal waveguiding [13] operating both pulsed and continuously is characterized by combining both laser outputs onto a whisker contact diode mixer mounted in a corner cube reflector. The resulting difference frequency beatnote is recorded in both the time and frequency domains. From the frequency domain data, we measure the effective laser linewidth and the tuning rates as a function of both temperature and injection. From the time domain data, we characterize the intra-pulse frequency tuning behavior, which limits the effective laser linewidth to ~5 MHz for 1 μs pulse width and measurement time.

Figure 1 shows the setup used to overlap the two QCLs onto a THz mixer. A 2 inch diameter f/1 gold coated off-axis parabolic (OAP) reflector (*Janos Technology* A8037P295) collimates the output of each laser. A beam combiner (BC) made out of a single 6 inch diameter 600μm thick polished wafer of high-resistivity silicon overlaps the beams with a reflection / transmission ratio of ~30 / 70%. A 3 inch diameter f/1 gold coated OAP (*Janos* A8037P316) then focuses the combined beams onto a *Farran Technology* CMB-5 corner cube mixer (CCM). This mixer is a whisker contact Schottky diode junction placed at the vertex of a gold coated corner cube [14,15] and has a specified operating frequency of 2 to 3 THz. Its radiation pattern overlaps optimally with an approximately f/1.8 horizontal incoming beam when the axis of the wire is collinear with the incoming beam and then pitched by ~24° above horizontal. A *Mini-Circuits* ZFBT-4R2G bias-tee connects directly to the SMA connectorized IF port of the CCM. A low-noise isolated dc supply provides the dc bias, typically ~0.3mA at 0.90V. An *AML Communications* AML0016L3801 ultra-broadband preamplifier (gain >38dB and noise figure <3.5dB from 10 to 6000 MHz) amplifies the ac part of the IF signal.

#116407 - $15.00 USD Received 28 Aug 2009; revised 16 Oct 2009; accepted 19 Oct 2009; published 23 Oct 2009

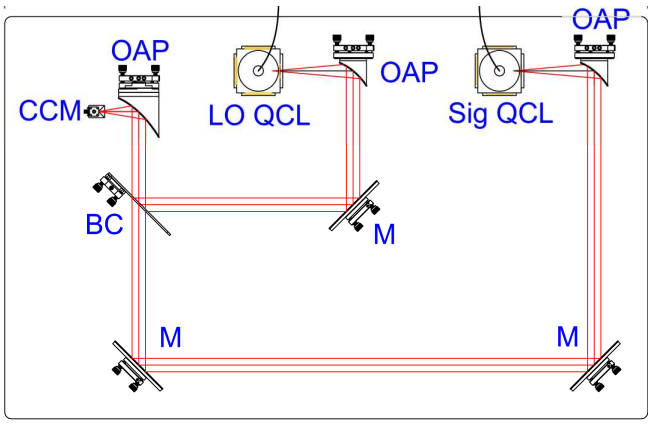

Fig. 1. Optical layout showing to scale the local oscillator (LO) and signal (Sig) quantum cascade lasers (QCL) mounted in their cryostats and directed with off-axis parabolic (OAP) reflectors, plane reflectors (M), and a beam combiner (BC) onto a corner cube mixer (CCM).

Variation with Laser Drive Current

The lasers can be driven either continuously (cw) or pulsed, typically 3 μs long pulses at 100 kHz. Initially, one laser was driven cw and the other pulsed at 100kHz with a 30% duty cycle square wave signal. Figure 2 shows the variation in the laser difference frequency as the cw current to laser "L1" is changed. In this experiment, laser 1 is operated cw and laser 2 ("M") is driven with 3 μs long pulses at 100 kHz. The spectrum analyzer observing the difference frequency beatnote is set for a 1.0 second sweep time and a 3 MHz resolution bandwidth. Besides the slight increase in signal size with increasing current for the smaller current values closer to laser threshold, the dominant effect is a change in output frequency. Fitting each of these individual spectra with a Gaussian, allows us to determine the center difference frequency, plotted as triangles in Fig. 2 as a function of laser drive current shown on the right axis. Fitting these current tuning results with a line gives a current tuning rate for the difference frequency. Since we are not measuring the absolute laser frequency, we cannot determine the absolute sign of the laser current tuning rate from these data alone,. However, from independent and much less precise measurements using an FTIR spectrometer, we conclude that the *laser* tuning rate has the same sign and is therefore also + 3775 ± 65 MHz/A.

Figure 3 shows the variation in the same laser difference frequency as the peak current to the pulse laser "M" is changed. Unlike the tuning behavior for the cw driven laser (Fig. 2), these spectra change in shape for different peak current values and in general become broader and more structured for larger currents. This occurs because the spectral output of the laser is changing during each pulse and from pulse to pulse. Note that the data recorded by the spectrum analyzer does not represent the average power at any specific frequency during the measurement time, but instead represents the peak power observed at each frequency sometime during the measurement interval. We apply the same Gaussian fit procedure to these data and plot the power weighted center frequency of each spectral output cluster as a function of peak current, as shown in Fig. 3. The resulting slope of the beatnote center frequency versus drive current indicates a current tuning rate of + 4968 ± 52 MHz/A for laser 2. We attribute the difference in current tuning rates between the two lasers to the fact that one laser is driven pulsed while the other is driven cw.

#116407 - $15.00 USD Received 28 Aug 2009; revised 16 Oct 2009; accepted 19 Oct 2009; published 23 Oct 2009

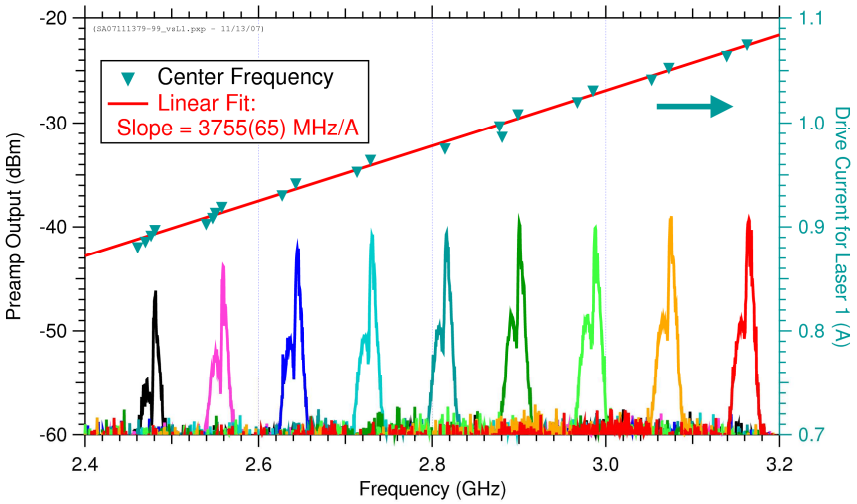

Fig. 2. Selected heterodyne signals between lasers A3264L1 (cw, T = 17 to 19K) and A3264M (pulsed 3μs at 100kHz, Peak Current = 763mA, T = 11K) for different drive currents applied to A3264L1. The triangles show the Gaussian fit center frequency of each spectrum plotted versus the drive current on the right axis. The associated linear fit indicates a laser tuning rate of 3755 ± 65 MHz/A.

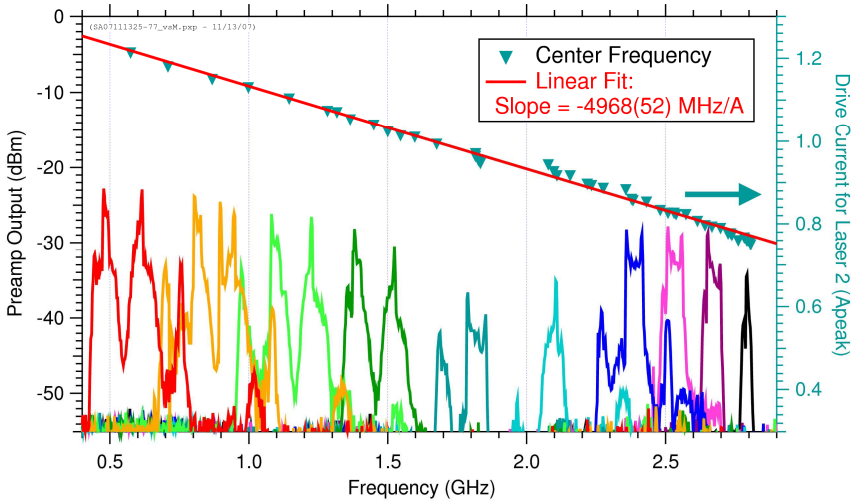

Fig. 3. Heterodyne signals between lasers A3264L1 (cw, T = 15K, Current = 966mA) and A3264M (pulsed 3μs at 100kHz, T = 9 to 17K) for different peak drive currents applied to A3264M. The triangles show the Gaussian fit center frequency of each spectrum plotted versus the drive current on the right axis. The associated linear fit indicates a laser tuning rate of 4968 ± 52 MHz/A.

Variation with Laser Temperature

In addition to the laser current, we can also vary the laser's temperature directly by changing the temperature of the cryostat cold finger on which it is mounted. With the temperature of the pulsed laser fixed at 6.0K, Fig. 4 plots the laser difference frequency spectra for different temperatures of the cw laser, along with the fitted center frequency versus temperature of "L1" on the right axis. This temperature tuning empirically fits best with a quadratic dependence. Because of the laser material's coefficient of thermal expansion variation with temperature [16], the temperature tuning is not expected to be linear.

#116407 - $15.00 USD Received 28 Aug 2009; revised 16 Oct 2009; accepted 19 Oct 2009; published 23 Oct 2009

Figure 5 shows the analogous results when the temperature of the pulsed laser ("M") is varied. Note that both lasers tune with current in the opposite direction as they tune with temperature. Conventional understanding is that the effective index of the laser gain region in QCLs is independent of current. According to this reasoning, the only mechanism for tuning in THz QCLs is via temperature which changes the cavity length due to thermal expansion. If this were the only mechanism, then increasing the current which increases the local laser temperature would change the laser frequency in the same direction as increasing the temperature of the cryostat cold plate. Since the opposite is observed, there must be another mechanism governing the current tuning which dominates this temperature effect.

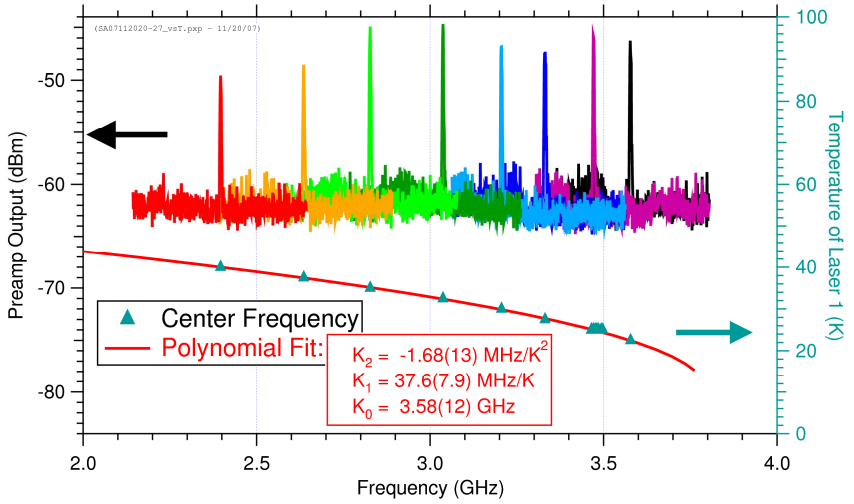

Fig. 4. Heterodyne signals between lasers A3264L1 (cw, Current = 1.180A) and A3264M (pulsed 3μs at 100kHz, Peak Current = 760mA, T = 6.0K) for different temperatures of A3264L1. The triangles and associated quadratic fit show the Gaussian fit center frequency of each spectrum plotted versus the laser temperature on the right axis.

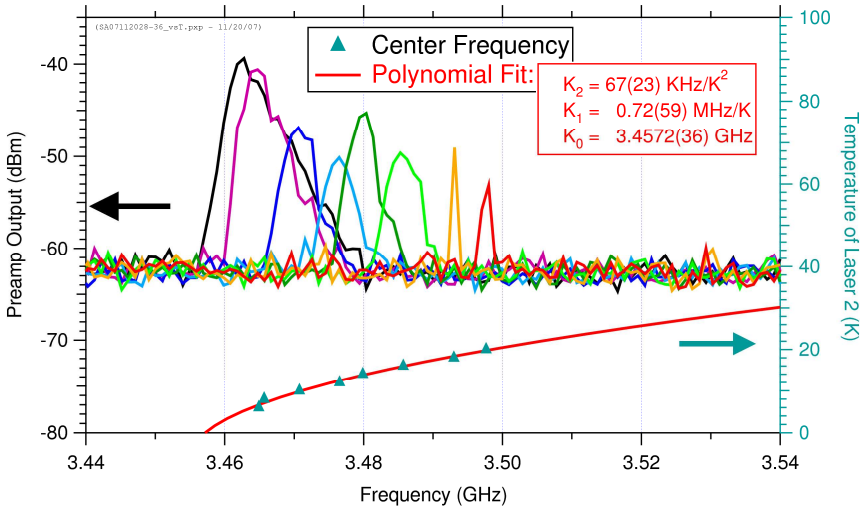

Fig. 5. Heterodyne signals between lasers A3264L1 (cw, Current = 1.180A, T = 25.0K) and A3264M (pulsed 3μs at 100kHz, Peak Current = 760mA) for different temperatures of A3264M. The triangles and associated quadratic fit show the Gaussian fit center frequency of each spectrum plotted versus the laser temperature on the right axis.

#116407 - $15.00 USD Received 28 Aug 2009; revised 16 Oct 2009; accepted 19 Oct 2009; published 23 Oct 2009

Heterodyne Signal in the Time Domain

Because of the relatively more complex output spectra we observe when we operate the lasers in pulsed mode, we used a sampling oscilloscope (*Tektronix* TDS6124C) with a 12 GHz bandwidth, fast enough to directly observe the 0 to 6 GHz heterodyne beat signal. Figure 6 shows the time and frequency domain of a single pulse. As above, laser 1 (L1) is on cw, while the second laser (M) is pulsed on for 3μs every 10μs (30% duty cycle). Because there are so many points in this 4μs record (4μs sampled at 10GHz = 40,000 points), the ~3 GHz heterodyne difference frequency oscillations appear as a solid blur (blue trace in top graph). Only the pulse envelope identified by the "Gate" trace along with lower frequency ringing at the beginning and end of the pulse is visible.

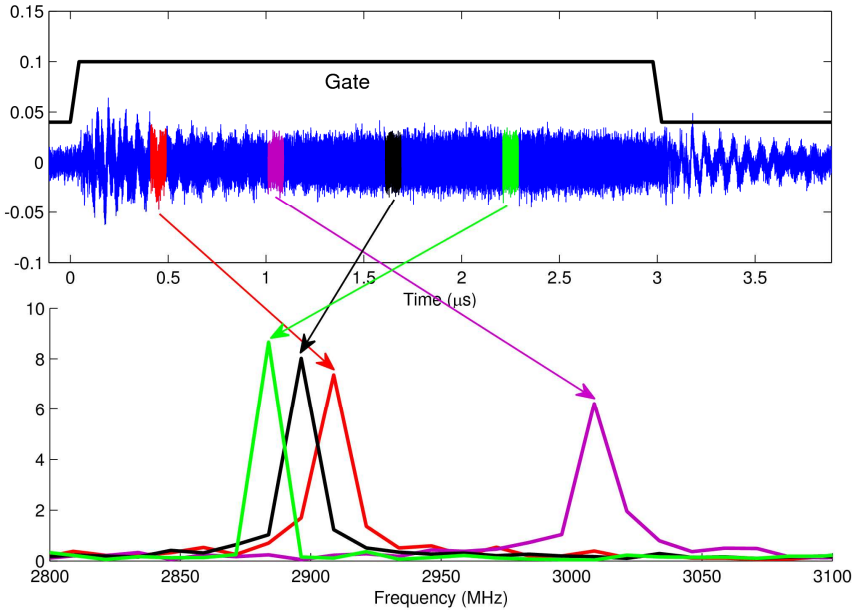

Fig. 6. Heterodyne signal between lasers A3264L1 (cw) and A3264M (pulsed) in the time (top) and frequency (bottom) domain. The pulsed laser turns on for 3μs every 10μs, as shown by the "Gate" trace. The FFT of 4 separate 80ns time segments are shown in the lower graph.

To watch the laser's spectral behavior during the pulse, the time domain data are broken into contiguous 50% overlapping 80ns long segments, four of which are highlighted in the top graph. The fast Fourier transform (FFT) of each of these segments is computed and the location of the spectral peak is noted. Four of these transformed data segments are shown in the lower graph.

Figure 7 shows the peak beatnote frequency as a function of time within the pulse for increasing drive current applied to the pulsed laser. These are the first observations of intra-pulse tuning in THz QCLs that we are aware of. At present, we do not fully understand the mechanism controlling this behavior, but can make some general observations. The intra-pulse behavior is perhaps best understood by reviewing the data acquired at the highest peak current (837mA, bottom curve), when the beatnote is present during the entire pulse. These red circles in Fig. 7 show a continuous variation in the beatnote center frequency which we attribute to a continuous variation in the laser center frequency. This variation is not monotonic and resembles the ringing that we have observed in other laser injection current pulses. This implies that the instantaneous laser frequency may be affected by the instantaneous carrier density in the gain medium. With lower peak current values, this continuous behavior is sometimes observed, but we also observe cases where the laser output

#116407 - $15.00 USD Received 28 Aug 2009; revised 16 Oct 2009; accepted 19 Oct 2009; published 23 Oct 2009

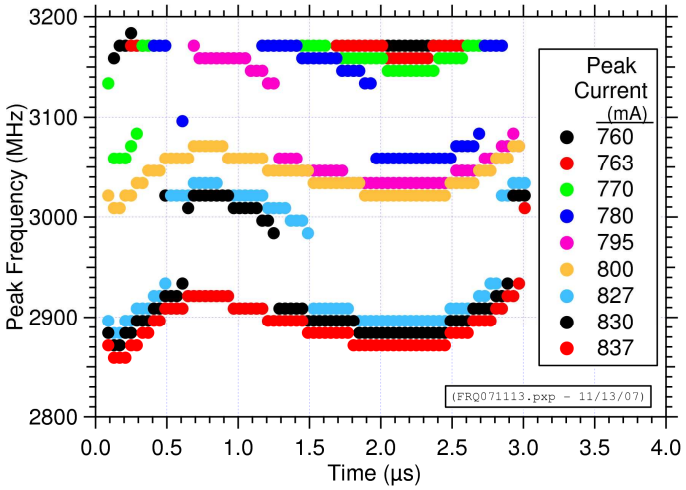

Fig. 7. Location of the peak frequency component versus time within a 3 µs long pulse for increasing drive current to the pulsed laser.

frequency jumps by a fixed amount of 100 MHz, to a different set of modes. There are also portions of some data sets where no beatnote is present. Since we know from homodyne measurements of this laser under the same conditions that the laser is on (i.e. emitting light), the lack of beatnote at these times indicates that the beat frequency must be outside of the 6 GHz range of the mixer + bias tee. These dropout periods are repeatable. Lastly, we observe that the sign of the laser current tuning rate is the same as shown in Fig. 4. To rule out the possibility that this tuning behavior is the result of optical feedback from multiple reflections in the optical setup, we repeated these measurements with an optical attenuator (10% transmission) in front of each laser. Identical tuning results were observed with attenuators in front of either or both lasers.

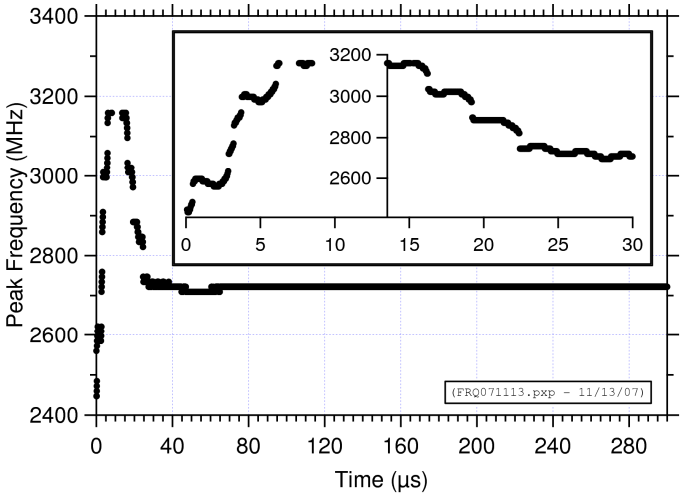

Fig. 8. Location of the peak frequency component versus time within a 919mA high (peak) 300µs and 30µs (inset) long pulse

Figure 8 show the analogous time evolution of the laser frequency for a 30 and 300 µs long pulse, respectively. It is possible that this ~800 MHz peak-to-peak frequency swing lasting ~30 µs arises from a real overshoot in the current applied to the laser by the pulser electronics. However, by monitoring the voltage across a sense resistor in series with the laser indicates that there is no such current overshoot, particularly on the 30 µs timescale. These

#116407 - $15.00 USD Received 28 Aug 2009; revised 16 Oct 2009; accepted 19 Oct 2009; published 23 Oct 2009

data most likely demonstrate the transient thermal effect of applying a rectangular pulse of current to the laser [17,18]. These measurements indicate that this thermal effect lasts less than 30 μs.

Heterodyne Bandwidth and Linewidth

By turning down the drive current to the pulsed laser, we can optimize the configuration for minimum laser linewidth. Figure 9 shows a beatnote with a 1/*e* halfwidth of 3.2 MHz, equivalent to a FWHM of 5.2 MHz, measured over the 100 ms sweep interval of the spectrum analyzer. This width is a convolution of the spectral widths of the two lasers and the resolution of the spectrum analyzer. The spectrum analyzer's resolution bandwidth is 1 MHz, and therefore negligibly affects this linewdith measurement. As discussed above, this beatnote linewdith is dominated by the intra-pulse tuning behavior of the pulsed laser.

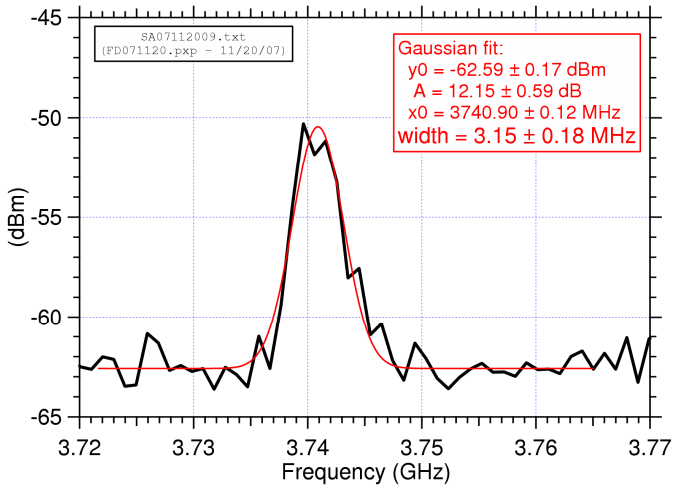

Fig. 9. Heterodyne signal between lasers A3264M (pulsed) and A3264L1 (cw) along with a Gaussian fit shown in red.

Conclusions

Using a room temperature heterodyne technique, we have characterized the spectral and tuning behavior under both pulsed and cw operation of 2.5 THz QCLs based on the chirped superlattice design with semiconductor-metal waveguiding. From the time domain data, acquired with a fast oscilloscope, mode hops and intra-pulse tuning are evident. In the frequency domain, acquired by an RF spectrum analyzer, complex spectra result from both the intra- and inter-pulse variations in the pulsed laser's output frequency. For small laser drive currents just above threshold, these broadening effects can be minimized to achieve an effective linewidth of approximately 5 MHz. The observed laser tuning rate versus current and temperature have opposite sign, indicating an additional tuning mechanism beyond the conventional temperature dependence on the laser's cavity length.

#116407 - $15.00 USD Received 28 Aug 2009; revised 16 Oct 2009; accepted 19 Oct 2009; published 23 Oct 2009